

G. GUMIENNY\*

**CARBIDIC BAINITIC AND AUSFERRITIC DUCTILE CAST IRON****ŻELIWO SFEROIDALNE BAINITYCZNE I AUSFERRYTYCZNE Z WĘGLIKAMI**

This article presents new kinds of carbidic ductile cast iron with different microstructures of the metal matrix. This cast iron was obtained using the Inmold method nodularisation which guarantees strong refining of graphite and the metal matrix components. A different microstructure of the metal matrix of the cast iron was obtained without any thermal treatment (unwrought) by a suitable composition of alloy additives. It was shown that by adding molybdenum, chromium, nickel and copper it is possible to obtain in the cast iron metal matrix consisting of upper bainite, its mixture with lower bainite or ausferrite in the casts with the wall thickness of 3÷25 mm. The process of cast iron crystallization is presented and described with the help of the thermal and derivative analysis (TDA) curves. It also shows the thermal effects from transformation of austenite in solid state.

*Keywords:* Carbidic Ductile Cast Iron, Bainite, Ausferrite, Thermal and Derivative Analysis (TDA)

W artykule przedstawiono nowe rodzaje żeliwa sferoidalnego z węglkami o różnej mikrostrukturze osnowy metalowej. Żeliwo to otrzymano stosując sferoidyzację metodą Inmold, zapewniającą dużą liczbę kulek grafitu i rozdrobnienie składników osnowy metalowej. Różną mikrostrukturę osnowy metalowej żeliwa otrzymywano bez stosowania obróbki cieplnej (w stanie surowym) poprzez odpowiednią kombinację ilościową dodatków stopowych. Wykazano, że dodatek molibdenu, chromu, niklu i miedzi w żelwie sferoidalnym pozwala uzyskać osnowę metalową złożoną z bainitu górnego, jego mieszaniny z dolnym lub ausferrytu w odlewach o grubości ściany 3÷25 mm. Proces krystalizacji żeliwa przedstawiono i opisano za pomocą krzywych analizy termicznej i derywacyjnej (ATD). Pokazano efekty cieplne od przemiany austenitu w stanie stałym.

**1. Introduction**

The dynamic technical progress sets clear requirements to the materials used for production of machine and device elements. It creates a necessity to work out and use new materials with high mechanical and application properties. It also concerns the ductile cast iron whose world production in 2010 was 22.6 million tons and constituted 25% of the world cast production [1]. In comparison to the previous year it increased by 3.2 million tons. It speaks to the fact that this material is still one of the most eagerly used by material engineers for machine and device elements.

At present the most wear resistible ductile iron is ADI. The microstructure of the metal matrix of this cast iron consists of ausferrite which is the mixture of bainitic ferrite and austenite in the quantity up to 40%. It is obtained using thermal treatment of the casts based on austenitizing and further austempering in the range of temperatures of about 250÷400°C [2].

The bainitic and ausferritic microstructure can also be obtained without using any thermal treatment (unwrought) using a suitable composition of the alloy additive [3÷5]. This technology is however less investigated. Such elements as Mo, Cr,

Ni and Cu influence, with different intensity, on the austenite stability in the pearlitic and bainitic range, that is why their suitable composition enables obtaining the metal matrix in ductile cast iron consisting of upper bainite, its mixture with lower bainite or ausferrite during continuous cooling. In bainite, unlike ausferrite, there are carbides separated from the carbon-saturated austenite and ferrite. It is also possible to obtain in cast iron carbides precipitated from a liquid which increases its wear and adhesive wear resistance [6].

In connection with the abovementioned the aim of the current work was to present the possibilities of obtaining of the bainitic and ausferritic microstructure in ductile cast iron by introducing molybdenum, chromium, nickel and copper. The process of cooling and crystallization was shown using the TDA curves. It was stated that it was possible to register the thermal effect when austenite was transforming into upper bainite or ausferrite.

**2. The methodology of the research**

The original cast iron was melted in the inductive furnace type PI 30 by Elkon with the frequency 3.8 kHz and capacity of 30 kg. The furnace charge was a pig iron with

\* DEPARTMENT OF MATERIALS ENGINEERING AND PRODUCTION SYSTEMS, TECHNICAL UNIVERSITY OF ŁÓDŹ, 1/15 STEFANOWSKIEGO STR., 90-924 ŁÓDŹ, POLAND

the chemical composition presented in Table 1 and scrap iron from S235JR steel with the chemical composition according to PN-EN 10025:2002U norm.

TABLE 1

The chemical composition of the pig iron

Chemical composition, wt. %				
C	Si	Mn	P	S
4.44	0.69	0.025	0.046	0.009

The content of silicon and manganese was regulated by additives of FeSi75 and FeMn75 correspondingly. Technically pure: Cr, Mo, Ni and Cu were used as alloy additives.

The chemical composition of the cast iron was tested in the emissive spectrometer with the spark excitation SPECTROMAXx by SPECTRO Analytical Instrument GmbH. The tested cast iron was divided into four groups differing by its chemical composition which is presented in Table 2.

TABLE 2

The chemical composition of the separate groups of the tested cast iron and their eutectic carbon equivalent  $C_e$  and the eutectic saturation coefficient  $S_c$

Group No	Chemical composition, wt. %							$C_e$ , wt. %	$S_c$
	C	Si	Mn	Mo	Cr	Cu	Ni		
I	3.45÷	2.41÷	0.20÷	-	-	-	-	4.19÷	0.98÷
	3.64	2.52	0.29						
II	3.30÷	2.37÷	0.06÷	1.98÷	-	-	0.66÷	4.03÷	0.94÷
	3.86	2.61	0.10	2.11			1.12	4.70	1.10
III	3.27÷	2.21÷	0.07÷	1.89÷	-	-	1.46÷	4.00÷	0.94÷
	3.93	2.63	0.09	2.08			1.74	4.81	1.13
IV	3.30÷	2.27÷	0.29÷	1.39÷	0.48÷	1.03÷	-	4.03÷	0.95÷
	3.75	2.56	0.34	1.55	0.54	1.54			

The average concentration of P and S in the cast iron was 0.04% and 0.01% correspondingly. The content of Mg in the casts was within the range of 0.04÷0.06%.

The eutectic saturation coefficient was calculated according to the formula:

$$S_c = \frac{C_c}{C_{eut}} = \frac{C_c + 0.31 \cdot Si - 0.027 \cdot Mn - 0.063 \cdot Cr + 0.074 \cdot Cu + 0.053 \cdot Ni - 0.015 \cdot Mo}{C_{eut}} \quad (1)$$

where:

- $C_c$  - complete content of carbon in the cast iron, wt. %,
- $C_{eut}$  - carbon content in the eutectic according to the stable system, wt. %.

The nodularisation of the cast iron was carried out by Inmold method. The scheme of the bench for cast iron nodularisation and TDA curves registration is shown in Figure 1.

The master alloy (5) is placed in the reaction chamber (4) situating in the ingate system behind the pouring gate (3). The chemical composition of the master alloy is given in Table 3. Behind the chamber there was a mixing chamber (6) which enabled precise dilution of the master alloy and its mixing with the components of the cast iron. The reaction chamber and the mixing chamber were sphere-like which guaranteed

the highest outcome of magnesium [7]. Then the cast iron filled the cavity in the shape of the sample cast (7) with the dimensions presented in Figure 2. When the cavity was filled, the cast iron through the overflow hole (8) left the mold and flooded the TDA standard probe (9) placed on the support (13). In the thermal device of the probe there was a PtRh10-Pt thermoelement (10) in the quartz tube shielding body (11) to register the temperature changes of the cast iron. The thermoelement was connected by a compensating cable (12) with the U/f converter and the latter with the computer. It enabled registration of the thermal  $t = f(\tau)$  and derivative  $dt/d\tau = f'(\tau)$  analyses curves. The curves were used to describe the process of the cast iron crystallization. The cooling rate of the cast iron in the TDA probe corresponded to the cooling rate of the sample cast with the wall thickness 12 mm.

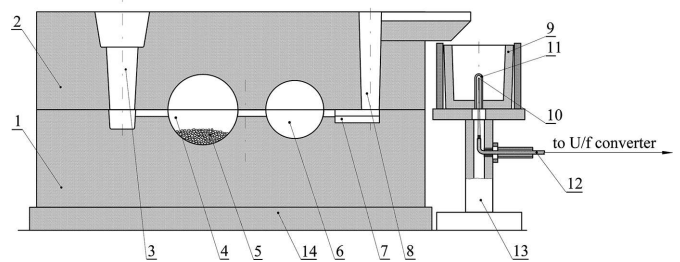


Fig. 1. The scheme of the bench for cast iron nodularisation and TDA curves registration: 1 – lower part of the mold, 2 – upper part of the mold, 3 – pouring gate, 4 – reaction chamber, 5 – master alloy, 6 – mixing chamber, 7 – sample cast, 8 – overflow hole, 9 – TDA probe, 10 – thermoelement PtRh10-Pt, 11 – thermoelement shield, 12 – compensating cable, 13 – support, 14 - base

TABLE 3

The chemical composition of the master alloy

Chemical composition, wt. %				
Si	Mg	Ca	RE*	Al
40.0÷49.0	3.0÷6.5	0.3÷1.0	0.3÷1.4	0.5÷1.2

\* - rare earth elements.

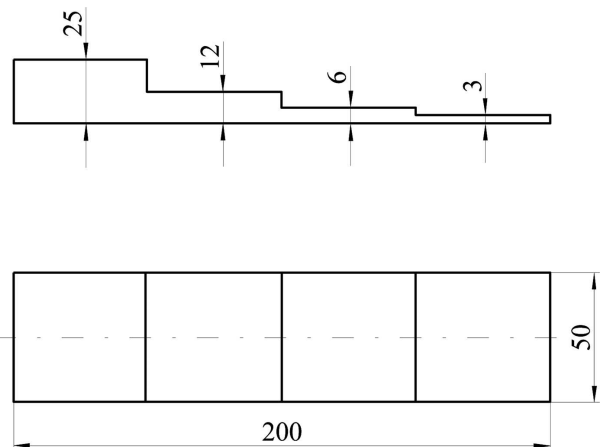


Fig. 2. The shape and dimensions of the sample cast

The microstructure of the cast iron was tested on the polished sections etched by nital magnified  $\times 200$  and  $\times 1000$  on the metallographic microscope Eclipse MA200 by Nikon.

The surface percent of the metal matrix components was tested using the NIS-Elements BR software for picture analysis.

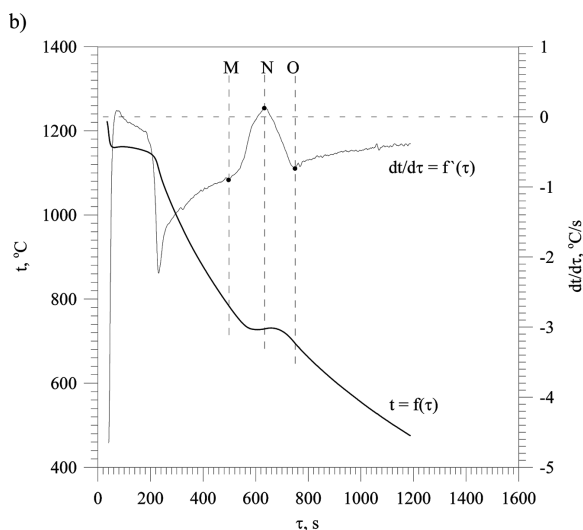
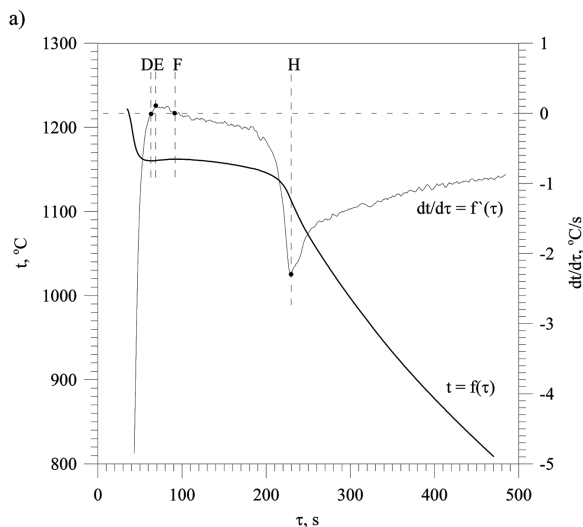
### 3. The research results

#### 3.1. Transformations which take place during crystallization and cooling of ductile cast iron

##### 3.1.1. Non-alloy ductile cast iron crystallization

In order to estimate the influence of the alloy additives on the temperature of the phase transformations and microstructure of the cast iron on the basis of the TDA curves non-alloy cast iron was analyzed (group I, Tab. 2).

In connection with this, Figure 3 (a÷d) presents the representative TDA curves (a, b) and microstructure (c, d) of ductile cast iron with the composition: 3.64% C; 2.56% Si; 0.33% Mn.



Point	$\tau$ , s	$t$ , °C	$dt/d\tau$ , °C/s
D	63	1160	–
E	69	1161	0.11
F	91	1162	–
H	230	1113	-2.30
M	497	785	-0.90
N	633	729	0.12
O	750	695	-0.74

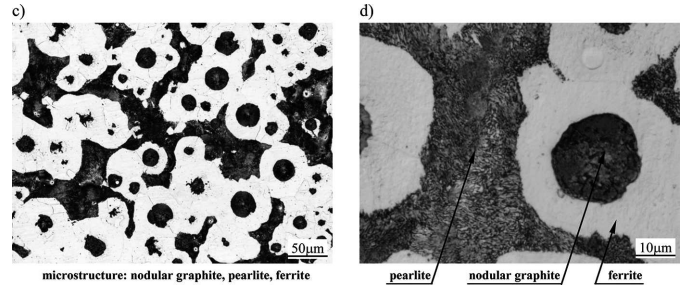


Fig. 3. (a÷d). The TDA curves (a, b) and the microstructure (c, d) of ductile cast iron with the chemical composition: 3.64% C; 2.56% Si; 0.33% Mn

It follows from the chemical composition analysis that it is hypereutectic cast iron ( $C_e = 4.57\%$ ), however, on the derivative curve there is no thermal effect from the initial graphite crystallization. This phenomenon is described in more details in the work [8]. The DEFH thermal effect comes from the crystallization of the austenite + nodular graphite eutectic. The temperature recalcence is  $2^\circ\text{C}$ . At the temperature of  $1113^\circ\text{C}$  (point H, Fig. 3a) the cast iron finishes crystallization and its microstructure consists of nodular graphite and austenite.

It follows from Fig. 3b that at the temperature of  $785^\circ\text{C}$  (point M) the transformation starts in the solid state. The high temperature shows that it starts from the  $\gamma \rightarrow \alpha + C_{gr}$  transformation. Maximum liberation of heat due to austenite transformation takes place at the temperature of  $729^\circ\text{C}$  (point N, Fig. 3b). The transformation ends at the temperature of  $695^\circ\text{C}$  (point O, Fig. 3b). It follows from Fig. 3c that after cooling to the ambient temperature the microstructure of the cast iron consists of nodular graphite, ferrite and pearlite. Regarding the small cooling rate of the cast iron in the TDA probe, a double thermal effect from the  $\gamma \rightarrow \alpha + P$  (pearlite) transformation is not noticed. The surface percent of the ferrite in cast iron matrix after the end of the crystallization process is about 55%.

##### 3.1.2. Carbide ductile cast iron crystallization

As it was mentioned, in order to obtain bainite or ausferrite in cast iron without using thermal treatment it is necessary to introduce the alloy additives which, when dissolved in austenite, have an influence on its hardness. To obtain upper bainite in the metal matrix a proper combination of molybdenum and nickel should be used. In connection with this, Figure 4 (a÷d) presents the representative TDA curves and microstructure of the ductile cast iron with upper bainite and carbides from group II (Tab. 2). In Table 4 the values describing the characteristic points in the TDA curves of studied types of ductile cast iron with carbides and obtained type of metal matrix microstructure are presented.

The chemical composition shows that this is slightly hypo-eutectic ( $C_e = 4.20\%$ ) and that is why its crystallization starts from forming of austenite seeds and their further growth, it is seen in the derived curve  $dt/d\tau = f'(\tau)$  in the form of a thermal effect described by points AB (Fig. 4a).

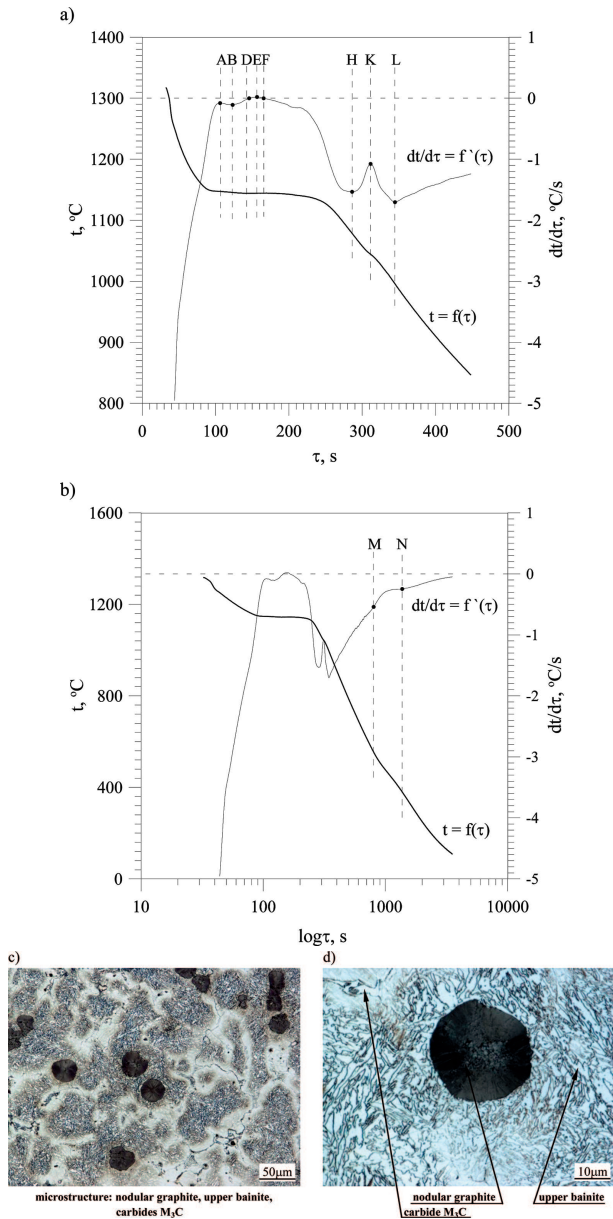


Fig. 4. (a÷d). The TDA curves (a, b) and microstructure (c, d) of carbidic ductile cast iron with the chemical composition: 3.46% C; 2.39% Si; 0.07% Mn; 2.13% Mo; 0.66% Ni

Then, within the temperature range of  $1145 \div 1078^\circ C$  the eutectic mixture consisting of austenite and nodular graphite crystallizes (thermal effect BDEFH, Fig. 4a). The synergic additive Mo and Ni caused a decrease in the temperature of eutectic crystallization in relation to the non-alloy cast iron by about  $15^\circ C$ . Carbides  $M_3C$  form after the end of eutectic  $\gamma +$  graphite crystallization. It is caused by simple microsegregation of molybdenum whose atoms are “moved” by the dendrites of austenite and eutectic cells front. For this reason the last portions of the liquid cast iron are enriched with molybdenum, so the tendency of the cast iron to crystallization increases according to the metastable system. On the crystallization curve the thermal effect is caused by the carbides crystallization described by the HKL points. The cast iron finishes its crystallization at the temperature of  $996^\circ C$  (point L, Fig. 4a). The microstructure of the cast iron at this temperature consists of nodular graphite, austenite and carbides placed on the borders on the eutectic cells.

A certain quantity of Mo dissolved in the austenite during cooling precipitates in the form of carbide  $Mo_2C$  as a result of variable dissolving of the Mo in the austenite. The remaining quantity of the molybdenum causes a significant increase in the austenite stability within the range of pearlite transformation and insignificant in the bainitic zone. In connection with this, at the temperature of  $554^\circ C$  the transformation  $\gamma \rightarrow B_U$  (upper bainite) starts (point M, Tab. 4, group III). In order to underline the thermal effect from this transformation the time axis is presented in the logarithmic system. The thermal effect from the  $\gamma \rightarrow B_U$  transformation ends at the temperature of  $380^\circ C$ . At the room temperature the microstructure of the cast iron situated in the TDA probe and containing about 2.0% Mo and 0.7% Ni consists of nodular graphite, upper bainite and carbides  $M_3C$ . Regarding a different cooling rate of certain walls of the sample cast the surface percent of the carbides changed from about 12 to 4% correspondingly in the 3 and 25 mm walls.

Figure 5 (a, b) presents the microstructure of carbidic ductile cast iron containing about 2.0% Mo and 1.5% Ni (group III, Tab. 2).

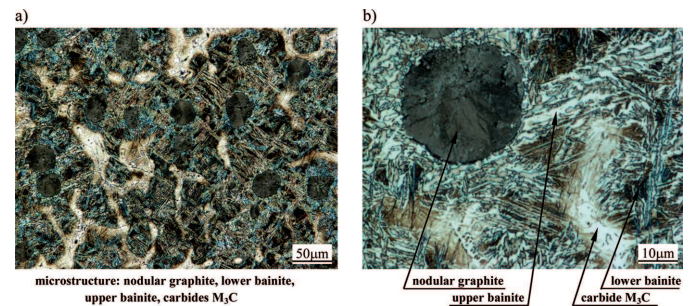


Fig. 5. (a, b). The microstructure of carbidic ductile cast iron with the chemical composition: 3.80% C; 2.52% Si; 0.08% Mn; 2.00% Mo; 1.48% Ni

Regarding the fact that this cast iron is hypereutectic ( $C_e = 4.62\%$ ), its crystallization starts from formation in the liquid iron of the graphite seeds whose size is bigger than the critical and their further growth in the form of the balls. Similar to the non-alloy cast iron the thermal effect from this process does not happen. The DEFH points described the thermal effect from the crystallization of the  $\gamma + C_{gr}$  eutectic. The increase in the carbon and nickel content with the similar concentration of molybdenum caused an increase in the temperature of the end of eutectic crystallization by  $22^\circ C$  (point H, Tab. 4, group III). It is caused by their graphitization process. Carbides  $M_3C$  crystallized within the temperature range of  $1100 \div 1001^\circ C$  (points HKL, Tab. 4, group III). Within the temperature range of  $529 \div 377^\circ C$  there is a slight thermal effect coming from the austenite transformation (points M and N, Tab. 4, group III). A bigger concentration of nickel in comparison to the previously described cast iron caused a significant decrease in the temperature of the beginning of the  $\gamma \rightarrow B_G$  transformation (by about  $40^\circ C$ ). It follows from the presented data that the increase of the nickel and carbon concentration in the cast iron decreases the temperature of the beginning of the austenite  $\rightarrow$  upper bainite transformation; however, it does not influence the temperature of this transformation end. A relatively high temperature in point N means that the thermal effect from the  $\gamma \rightarrow B_L$  (lower bainite) transformation



TABLE 4

The values for the characteristic points in the TDA curves of studied types of ductile cast iron with carbides and the corresponding microstructure

Point	The group of ductile cast iron The microstructure of metal matrix containing carbides								
	II upper bainite			III upper and lower bainite			IV ausferrite		
	$\tau$ , s	t, °C	dt/dr, °C/s	$\tau$ , s	t, °C	dt/dr, °C/s	$\tau$ , s	t, °C	dt/dr, °C/s
A	106	1147	-0,08	–	–	–	–	–	–
B	123	1145	-0,11	–	–	–	–	–	–
D	146	1144	–	83	1144	–	131	1141	–
E	157	1144	0,02	98	1146	0,16	149	1143	0,16
F	166	1144	–	123	1148	–	178	1146	–
H	286	1078	-1,53	249	1100	-1,49	302	1102	-1,53
K	311	1044	-1,07	288	1044	-0,99	362	1025	-0,69
L	345	996	-1,70	319	1001	-1,66	377	1009	-1,51
M	800	554	-0,54	841	529	-0,49	1175	459	-0,33
N	1371	380	-0,25	1333	377	-0,25	2067	283	-0,16

does not happen. It is caused by the fact that the transformation happens impulsively, that is why the thermolement, due to its inertia, is not able to register it. It follows from Fig. 5a, b that the microstructure of the metal matrix of the cast iron comprising about 2.0% Mo and 1.5% Ni consists of the mixture of upper and lower bainite and carbides placed on the borders of the eutectic cells. The surface percent of lower bainite is about 55%. The surface percent of carbides is from about 10 to 3% correspondingly in the wall 3 and 25 mm.

In the cast iron containing about 1.5% Mo adding of about 1.5% Cu and 0.5% Cr enables obtaining the ausferritic microstructure of the metal matrix without using thermal treatment. The microstructure of that kind of the cast iron (group IV, Tab. 2) are presented in Figure 6 (a, b).

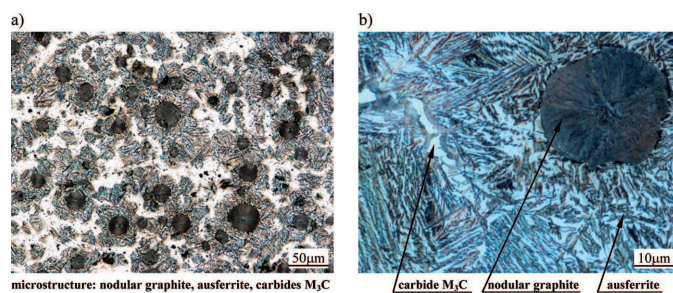


Fig. 6. (a, b). The microstructure of carbidic ductile cast iron with the chemical composition: 3.75% C; 2.40% Si; 0.33% Mn; 1.41% Mo; 0.51% Cr; 1.53% Cu

This cast iron is hypereutectic ( $C_e = 4.55\%$ ), that is why its crystallization starts from graphite precipitation from the liquid. Similarly, as in the previously described kinds of hypereutectic cast irons the thermal effect from this stage of crystallization was not registered. When the content of Cr is about 0.5% and 1.5% Mo precipitations of pre-eutectic carbide  $(Fe,Cr)_3C$  are not formed. The temperature of the eutectic transformation is close to the transformation in bainitic cast iron. As a result of enriching of the last portion of the liquid with molybdenum and chromium within the temperature range of  $1059 \div 1007^\circ\text{C}$  (points HKL, Tab. 4, group IV) carbides  $M_3C$  crystallize. It follows from Tab. 4 that the thermal effect MN occurs within the temperature range of  $459 \div 283^\circ\text{C}$ .

It comes from the  $\gamma \rightarrow \alpha_B$  transformation. When the crystallization process finishes, the microstructure of the cast iron consists of nodular graphite, ausferrite and carbides (Fig. 6a, b). Analogically, as in the previously described kinds of cast iron the quantity of carbides decreased when the wall thickness of the cast increases and was from about 10 to 4% in the 3 and 25 mm walls correspondingly.

#### 4. Conclusions

The research results presented in the current work enable coming to the following conclusions:

- the synergic additive of about 2.0% Mo and 0.7% Ni enable obtaining upper bainite and carbides in the unwrought metal matrix of ductile iron,
- an increase in the quantity of nickel to about 1.5% causes the austenite transformation into the mixture of upper and lower bainite in the casts with the wall thickness of  $3 \div 25$  mm,
- introduction of about 0.5% Cr, 1.5% Mo and 1.5% Cu to the cast iron enable obtaining ausferrite without using thermal treatment,
- on the derivative curve there is a thermal effect from the austenite transformation into upper bainite and ausferrite.

#### Acknowledgements

Scientific project financed from means of budget on science in years 2009÷2012 as research project N N508 411437

#### REFERENCES

- [1] 44<sup>th</sup> Census of World Casting Production, Modern Casting, 16-19, December 2010.
- [2] E. G u z i k, The processes of cast iron enrichment – selected problems, Archives of Foundry Engineering, 2001, Monograph No 1M [in Polish].
- [3] S. P i e t r o w s k i, Ductile iron with the structure of bainite with austenite or bainitic ferrite, Archives of Materials Science 4, 18, 253-273 (1997), [in Polish].

- [4] S. Pietrowski, G. Gumienny, Bainite obtaining in cast iron with carbides castings, Archives of Foundry Engineering **10**, 1, 109-114 (2010).
- [5] G. Gumienny, Chromium and copper influence on the nodular cast iron with carbides microstructure, Archives of Foundry Engineering **10**, 4, 47-54 (2010).
- [6] S. Pietrowski, G. Gumienny, Wear resistance of cast iron, Archives of Foundry Engineering **8**, 3, 173-180 (2008).
- [7] S. Pietrowski, Influence of reaction chamber shape on the cast-iron spheroidization process in-mold, Archives of Foundry Engineering **10**, 1, 115-122 (2010).
- [8] S. Pietrowski, G. Gumienny, B. Pisarek, T. Szymczak, R. Władysław, The analysis of the correctness of the estimation of crystallization of the chosen alloys by the TDA method, High Quality Casting Technologies, Materials and Casts, collective work under the editorship of Stanisław Pietrowski, pp. 111-132, Katowice – Gliwice 2011, [in Polish].

*Received: 10 April 2012.*